

LABORATORY RECORDS



3 4456 0050907 3

PHYSICS DIVISION

QUARTERLY PROGRESS REPORT

FOR PERIOD ENDING MARCH 20, 1951

DECLASSIFIED

CLASSIFICATION CHANGED TO:

BY AUTHORITY OF: E. J. Murphy 8.4.61

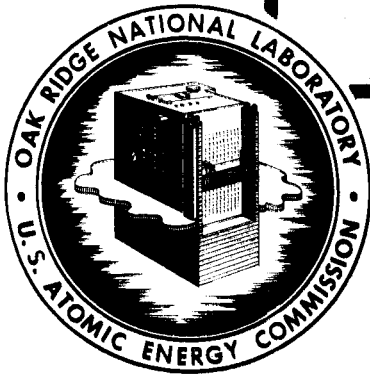
BY: S. Beadel 6.13.62

CENTRAL RESEARCH LIBRARY
DOCUMENT COLLECTION

LIBRARY LOAN COPY

DO NOT TRANSFER TO ANOTHER PERSON

If you wish someone else to see this document,
send in name with document and the library will
arrange a loan.



OAK RIDGE NATIONAL LABORATORY
OPERATED BY
CARBIDE AND CARBON CHEMICALS COMPANY
A DIVISION OF UNION CARBIDE AND CARBON CORPORATION



POST OFFICE BOX P
OAK RIDGE, TENNESSEE

ORNL-1006

This document consists of 41 pages.
Copy 9 of 168. Series A.

Contract No. W-7504, eng. 26

PHYSICS DIVISION

A. H. Snell, Director
E. O. Wollan, Associate Director

QUARTERLY PROGRESS REPORT
for Period Ending March 20, 1951

S. Bernstein, Editor



3 4456 0050907 3

DATE ISSUED: JUL 2 1951

OAK RIDGE NATIONAL LABORATORY
operated by
CARBIDE AND CARBON CHEMICALS COMPANY
A Division of Union Carbide and Carbon Corporation
Post Office Box P
Oak Ridge, Tennessee

This document
N
I

MARTIN MARIETTA

INTERNAL DISTRIBUTION

- | | | |
|------------------------------|-----------------------|-----------------------------|
| 1. G. T. Felbeck (C&CCC) | 23. A. H. Snell | 40. M. E. Rose |
| 2-3. Chemistry Library | 24. J. A. Swartout | 41. S. Bernstein |
| 4. Physics Library | 25. A. Hollaender | 42. G. E. Boyd |
| 5. Biology Library | 26. K. Z. Morgan | 43. Lewis Nelson |
| 6. Health Physics Library | 27. F. L. Steahly | 44. R. W. Stoughton |
| 7. Metallurgy Library | 28. M. T. Kelley | 45. C. E. Winters |
| 8-9. Training School Library | 29. W. H. Pennington | 46. W. H. Jordan |
| 10-13. Central Files | 30. E. O. Wollan | 47. E. C. Campbell |
| 14. C. E. Center | 31. D. W. Cardwell | 48. D. S. Billington |
| 15. C. E. Larson | 32. A. S. Householder | 49. M. A. Bredig |
| 16. W. B. Humes (K-25) | 33. L. D. Roberts | 50. R. S. Livingston |
| 17. W. D. Lavers (Y-12) | 34. J. A. Lane | 51. C. P. Keim |
| 18. A. M. Weinberg | 35. M. M. Mann | 52. J. L. Meem |
| 19. E. H. Taylor | 36. R. N. Lyon | 53. C. E. Clifford |
| 20. E. D. Shipley | 37. W. C. Koehler | 54. G. H. Clewett |
| 21. E. J. Murphy | 38. W. K. Ergen | 55. C. D. Susano |
| 22. F. C. VonderLage | 39. E. P. Blizzard | 56-61. Central Files (O.P.) |

EXTERNAL DISTRIBUTION

- 62-73. Argonne National Laboratory
- 74. Armed Forces Special Weapons Project
- 75-80. Atomic Energy Commission, Washington
- 81. Battelle Memorial Institute
- 82-85. Brookhaven National Laboratory
- 86. Bureau of Ships
- 87-88. Carbide and Carbon Chemicals Company (C-31 Plant)
- 89-90. Carbide and Carbon Chemicals Company (K-25)
- 91-94. Carbide and Carbon Chemicals Company (Y-12)
- 95. Chicago Patent Group
- 96. Chief of Naval Research
- 97. Columbia University (Havens)
- 98-100. duPont Company
- 101. H. K. Ferguson Company
- 102-105. General Electric Company, Richland
- 106. Hanford Operations Office
- 107-110. Idaho Operations Office
- 111. Iowa State College
- 112. Kellex Corporation
- 113-116. Knolls Atomic Power Laboratory
- 117-119. Los Alamos
- 120. Mallinckrodt Chemical Works
- 121-123. Mound Laboratory
- 124. National Advisory Committee for Aeronautics
- 125. National Bureau of Standards
- 126. Naval Medical Research Institute
- 127. Naval Research Laboratory

- 128. ~~New Brunswick Laboratory~~
- 129-130. ~~New York Operations Office~~
- 131-133. ~~North American Aviation, Inc.~~
- 134. ~~Patent Branch, Washington~~
- 135. ~~Sandia Corporation~~
- 136. ~~Savannah River Operations Office~~
- 137. ~~UCLA Medical Research Laboratory~~
- 138. ~~USAF - Headquarters~~
- 139. ~~U. S. Navy Radiological Defense Laboratory~~
- 140-144. ~~University of California Radiation Laboratory~~
- 145-146. ~~University of Rochester~~
- 147-150. ~~Westinghouse Electric Corporation~~
- 151-153. ~~Wright-Patterson Air Force Base~~
- 154-168. ~~Technical Information Service, Oak Ridge~~

Physics Division quarterly progress reports previously issued in this series are as follows:

ORNL 51	March, April, and May, 1948
ORNL 159	June, July, and August, 1948
ORNL 228	September, October, and November, 1948
ORNL 325	December, January, and February, 1948-49
ORNL 365	Period Ending June 25, 1949
ORNL 480	Period Ending September 25, 1949
ORNL 576	Period Ending December 15, 1949
ORNL 693	Period Ending March 15, 1950
ORNL 781	Period Ending June 15, 1950
ORNL 864	Period Ending September 20, 1950
ORNL 939	Period Ending December 20, 1950

Unclassified work for the period between November, 1948 and and December 20, 1950 is reported in the following reports: ORNL 325 Supplement, ORNL 366, ORNL 481, ORNL 577, ORNL 694, ORNL 782, ORNL 865, and ORNL 940.

TABLE OF CONTENTS

INTRODUCTION AND SUMMARY	6
1. CRITICAL EXPERIMENTS	8
2. SHIELDING MEASUREMENTS	12
Lid Tank	12
Activation of Sodium Shielded by B_4C	13
Biological Dose Behind B_4C - H_2O Shield	16
3. LIQUID-METAL DUCT TEST	36
4. BULK SHIELDING TEST FACILITY	37
5. ANP PHYSICS GROUP	38

LIST OF TABLES

Table		Page
1	Comparison of Na and Au Activation with BF_3 Counter Measurements in Solid B_4C	17
2	Neutron Attenuation of B_4C	19
3	Neutron Attenuation in H_2O Behind B_4C	22
4	Neutron Attenuation of $\text{B}_4\text{C}-\text{H}_2\text{O}$	23
5	Effect of Position of 12-in. B_4C Slab on Attenuation of $\text{B}_4\text{C}-\text{H}_2\text{O}$ Shield	25
6	Vertical and Horizontal Traverses in H_2O Behind B_4C in Dry Tank	28
7	Vertical Traverse Behind 20-in. B_4C Block in H_2O	29
8	Attenuation of $\text{B}_4\text{C}-\text{H}_2\text{O}$	31
9	Neutron Attenuation of $\text{B}_4\text{C}-\text{Fe}-\text{H}_2\text{O}$	33
10	Gamma Ray Attenuation of B_4C , Fe, and H_2O	35

LIST OF FIGURES

Fig.		
1	Apparatus for Critical Experiments	9
2	Typical Reactor Core Assembly	10
3	Comparison of Na, Au, and BF_3 Activation in Solid B_4C , Uncorrected Data	18
4	Neutron Attenuation, B_4C	20
5	Thermal Neutron Flux in H_2O Behind Several Thicknesses of B_4C , 25-in. BF_3 Counter	21
6	Effect of Position of 12-in. B_4C Slab on Attenuation of $\text{B}_4\text{C}-\text{H}_2\text{O}$ Shield	24
7	Vertical and Horizontal Traverses in H_2O Behind Dry Tank	26
8	Vertical Traverse Behind 20-in. Block in H_2O Voids Filled with Wood	27
9	Gamma Attenuation of $\text{B}_4\text{C}-\text{H}_2\text{O}$ Ion Chamber Measurements	30
10	Neutron Attenuation of $\text{B}_4\text{C}-\text{Fe}-\text{H}_2\text{O}$	32
11	Gamma Ray Attenuation of $\text{B}_4\text{C}-\text{Fe}-\text{H}_2\text{O}$	34

INTRODUCTION AND SUMMARY

This report covers classified work in the Physics Division for the period December 20, 1950 to March 20, 1951. The unclassified section of the Physics Division Quarterly Progress Report appears separately (ORNL-1005).

Critical Experiments

The purpose of the Critical Experiments program is to investigate properties of critical assemblies composed of uranium and various reflectors and moderators. During this quarter the installation of the equipment in the laboratory was completed. The critical experiment apparatus is described with accompanying photographs. Results with the first critical assembly composed of uranium with beryllium moderator are discussed. The observed critical masses differ appreciably from the calculated values. The possible causes for this discrepancy are being studied. Preliminary measurements of the effective energy for fission in the assembly have been made.

Shielding Measurements

Measurements of the neutron and gamma attenuation in solid B_4C followed by water have been made in the lid tank. Results are given for measurements of the following quantities:

1. Activation of Au foils and $NaNO_3$ samples in solid B_4C .
2. Neutron measurements in solid B_4C .
3. Attenuation of thermal neutrons in H_2O behind B_4C .
4. Comparison of B_4C attenuation at various distances from the source in H_2O .
5. Thermal neutron vertical and horizontal traverses behind various B_4C samples.
6. Gamma measurements in H_2O behind various thicknesses of B_4C .
7. Neutron attenuation of B_4C -Fe- H_2O .
8. Gamma attenuation of B_4C -Fe- H_2O .

Liquid-Metal Duct Test

A liquid-metal duct test is being conducted in the water tank on the vertical thermal column on top of the reactor. Neutron measurements in the water beyond the end of several lengths of duct are being taken with various detectors. The duct configurations are described.

Bulk Shielding Test Facility

The Bulk Shielding Test Facility program of calibrating instruments has been completed. The power calibration of the shielding reactor is about 75% complete. Centerline measurements in pure water are 90% complete. Fast-neutron measurements on an iron-water shield are planned before tests on the unit shield. Spectroscopic instruments for the divided shield measurements are being developed.

ANP Physics Group

The current activities of the ANP Physics Group are reported in detail in the ANP quarterly progress report, ANP-60. A short summary is given in this report. Results of calculations related to the ANP and ARE reactors are discussed.

1. CRITICAL EXPERIMENTS

A. D. Callihan

During the last quarter the installation of the equipment in the laboratory was completed; sufficient uranium and beryllium have been procured to begin experimentation late in this quarter.

The purpose of the program is to investigate the properties of critical assemblies composed of uranium and various neutron reflectors and moderators. Other materials, simulating structural members, coolants, etc. of the aircraft reactor, can be included in the assemblies. The mass of uranium required for criticality, the spectral and spatial distribution of neutrons within the array, and the effectiveness of controls are some of the variables to be examined as assembly components are changed.

The apparatus consists essentially of two matrices of 3-in.-square aluminum tubing 3 ft long, mounted on two tables, one being stationary and the other so arranged that it can be motor driven toward the first. Enriched uranium metal and the other materials under study as moderators, etc., are assembled in units approximately 3 in. square and of suitable length and are placed in the aluminum tubing. The two parts of the final array are then brought together by remote control. The usual safety and control rods, the latter for fine adjustment, are built into the assembly, and the approach to criticality is monitored with neutron and gamma detectors.

An overall picture of the apparatus is shown in Fig. 1; the movable table is on the left. The end of one-half of an assembly is shown in the top of the movable bundle of aluminum tubes and, of course, the other half is similarly placed in the fixed matrix. Four safety rods, the longer cylinders, and two control rods may be seen at the rear of each of the arrays. Attached to the fixed half, at the interface, is the motor drive for positioning the neutron source. Various neutron and gamma detectors are shown around the apparatus. Figure 2 is a close-up of one of the sets of aluminum tubes showing the interface of half an assembly. One of the elements, which is partly removed, consists of blocks of beryllium 1 in. thick with uranium disks between them, all strung on a horizontal rod. The source drive motor is at the top.

The uranium metal is being fabricated into disks approximately 3 in. in diameter and 0.010 in. thick by first rolling billets to the required thickness and then punching the disks. Since it has not been possible to roll to

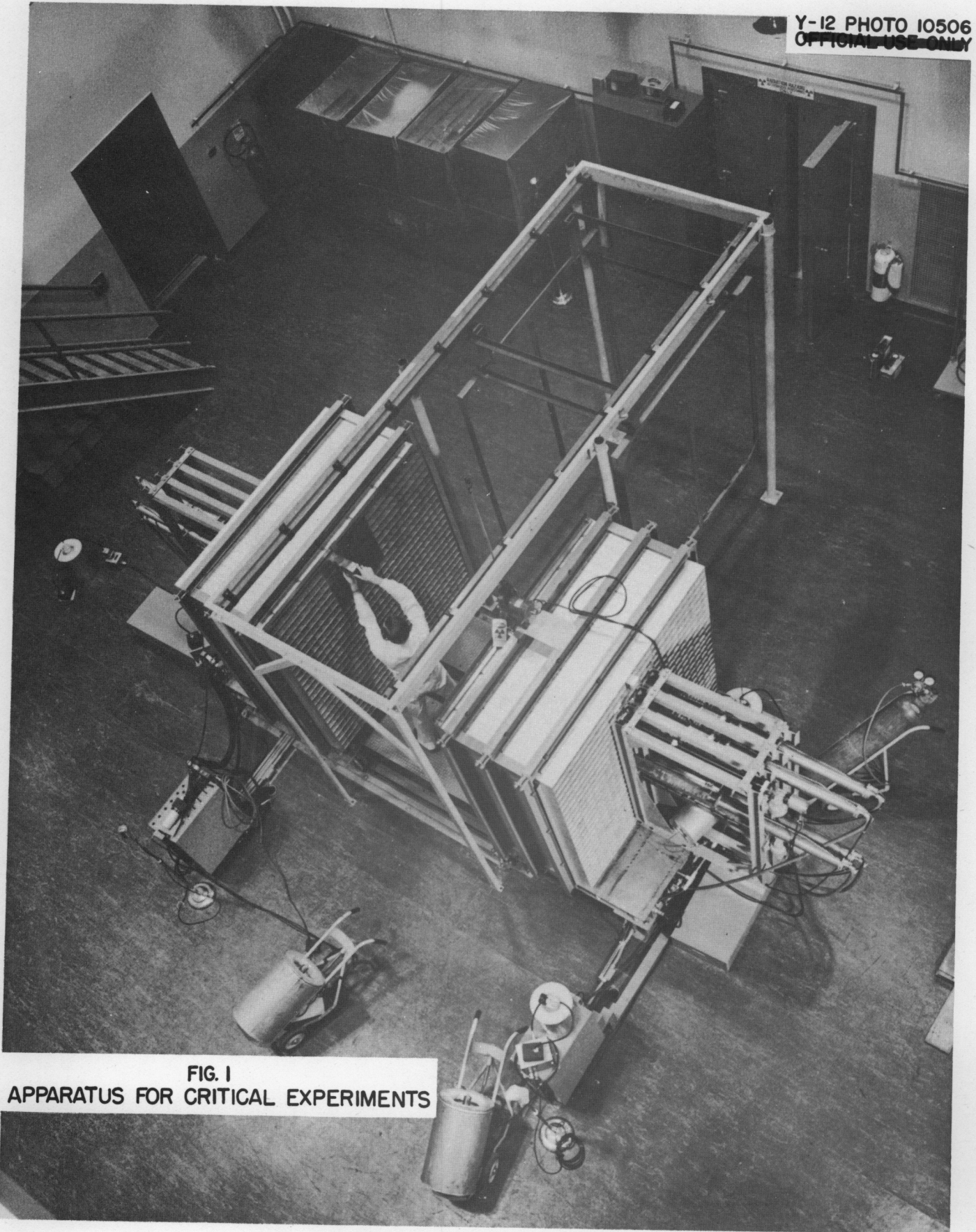
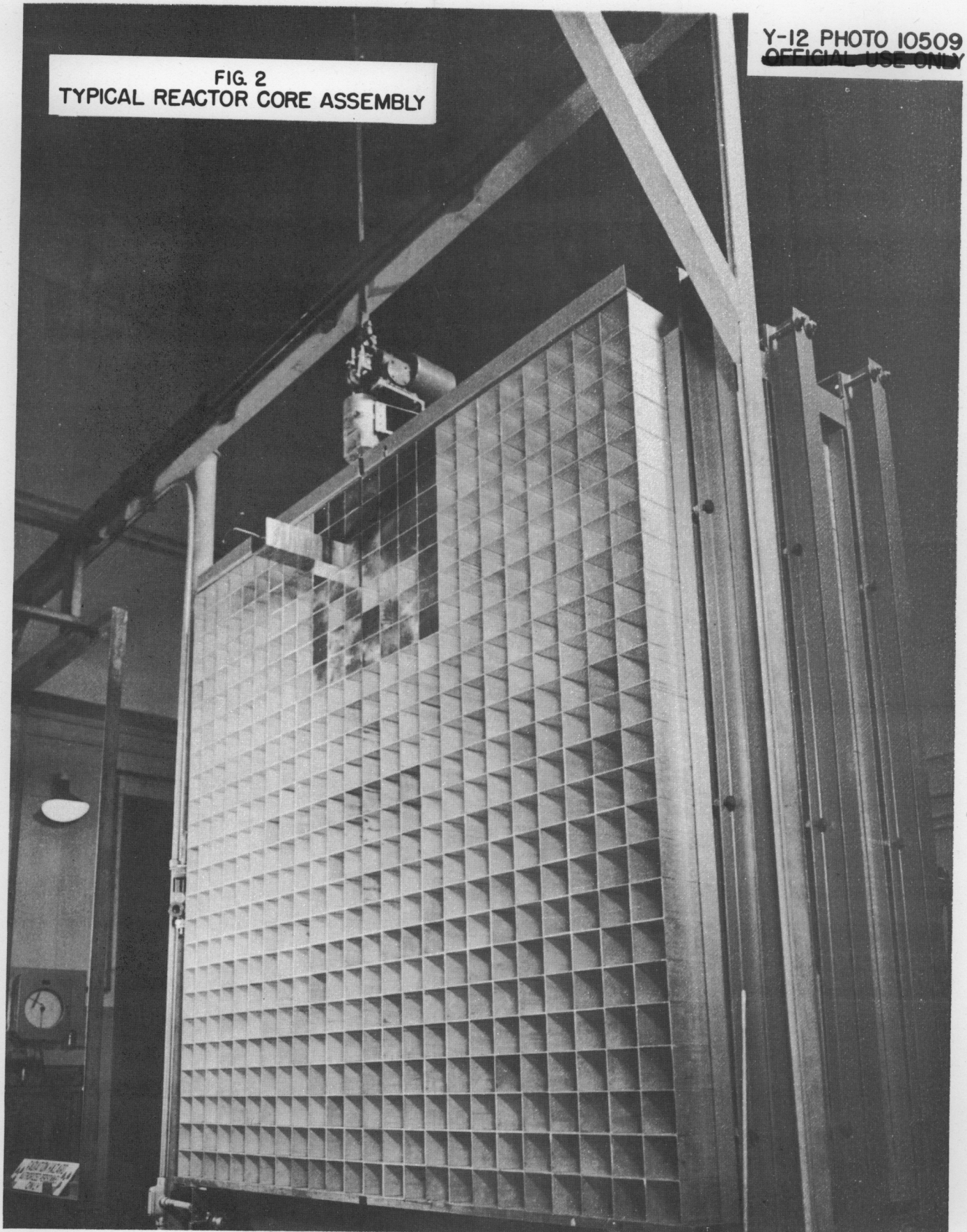


FIG. 1
APPARATUS FOR CRITICAL EXPERIMENTS

FIG. 2
TYPICAL REACTOR CORE ASSEMBLY



uniform thickness, the finished disks were brought to target weight by punching small holes in them. The 1200 disks in the first batch delivered were found to be heavily coated with black oxide, probably formed during hot rolling, which, because of its nonadherence, presented a severe contamination and accountability problem. The oxide was readily removed by leaching in concentrated nitric acid, after which the metal was kept at room temperature in an atmosphere of about 15% relative humidity. The oxide coating which is now being laid down is quite adherent. It has been necessary, however, to lower the target weight of all disks by about 5% because of the weight loss in the first batch during leaching.

The first critical assembly to be built was simple in structure in order that it would lend itself readily to calculation. It was to have beryllium metal as a moderator, to be cubical, and to have no reflector. In the procedure followed, an assembly of beryllium was first made with stepwise addition of uranium in the center. The Be/ U^{235} atomic ratio of the loaded elements was 386. Criticality was first achieved with about 6 kg of uranium in the core and a 6-in. layer of beryllium as a reflector. As more uranium was added the reflector was removed, resulting, finally, in an assembly 21 by 21 by 23 in., with no reflector, and containing about 18 kg of U^{235} , which was critical with one control somewhat removed leaving a small void near the center. Extrapolation to the condition of all rods in, i.e., no voids, gives 17.5 kg as the mass. The calculated values are 40 to 60% greater than those observed. Consequently, attempts have been made to ascertain if the discrepancy can be attributed to misinterpretation of the experiment, the most likely cause being spurious reflection of leakage neutrons back into the core by the supporting structure or by the concrete floor. No effect has thus far been found which will account for the difference.

Some very preliminary measurements on the activity induced in bare and cadmium-covered uranium foils at the center of the core shows the median energy for fission of the neutrons to be of the order of 0.5 ev. Estimates have also been made of the power level, which allow rough calibration of some of the instruments and a survey of personnel shielding.

2. SHIELDING MEASUREMENTS

C. E. Clifford	J. D. Flynn
E. P. Blizard	M. C. Marney
T. V. Blosser	F. K. McGowan

Lid Tank. During the past two quarters measurements of the neutron and gamma attenuation in solid B_4C followed by water have been made in the lid tank. Quantities of particular interest are the variation of the biological dose with the thickness of B_4C at the outer side of the B_4C - H_2O shield and the activation to be expected in a coolant (particularly sodium) located at various depths of the B_4C .

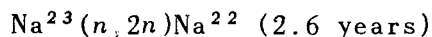
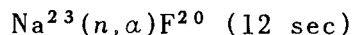
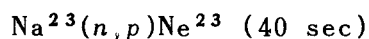
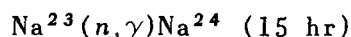
Following is a tabulation of the quantities which have been measured, with indication of the location of the data in this report:

QUANTITY MEASURED	DETECTOR	FIGURE NO.	TABLE NO.
Activation of Au foils and $NaNO_3$ samples in solid B_4C	Au foils, ~ 0.005 in., 6.45 cm ² ; $NaNO_3$ samples, 140 g	3 and 4	1 and 2
Neutron measurements in solid B_4C	25-in. BF_3 proportional counter jacketed with 1 to 3 in. of B_4C	3	1
Attenuation of thermal neutrons in H_2O behind B_4C	25-in. BF_3 proportional counter, bare	5	3 and 4
Comparison of B_4C attenuation at various distances from source in H_2O	25-in. BF_3 proportional counter in H_2O behind sample	6	5
Thermal neutron vertical and horizontal traverses behind various B_4C samples	8-in. BF_3 proportional counter	7 and 8	6 and 7
Gamma measurements in H_2O behind various thicknesses of B_4C	Ionization chamber	9	8
Neutron attenuation of B_4C -Fe- H_2O	25-in. BF_3 counter in H_2O behind sample	10	9
Gamma attenuation of B_4C -Fe- H_2O	Ionization chamber measurements in H_2O behind sample	11	10

The general method of shield measurement is the same as that which has been used for some time. A plate of uranium is irradiated by slow neutrons from the Oak Ridge reactor, and the resulting fission neutrons and gammas enter an adjacent large water tank. Samples to be measured are inserted in this lid tank and radiation is observed within or behind the sample. If it is necessary to keep samples dry, as is the case with the 1-in. B_4C slabs, a "dry tank" is appropriately placed in the lid tank and the samples are inserted in it.

The B_4C samples are in the form of one 20-in.-thick block, 5 by 4 ft, supplied by KAPL, and seventeen 1-in.-thick slabs, 5 by 4 ft, supplied by NEPA. The 20-in. block contains B_4C of density 1.95 g/cc plus 0.135 g/cc of occluded H_2O . The NEPA slabs have an average density of B_4C of 1.8 g/cc, are clad in 0.315 cm of aluminum, and are less than 0.5% water by weight. See ORNL-858 for a more complete description of the samples.

Activation of Sodium Shielded by B_4C . The exposure of sodium to a fast-neutron flux is known to lead to the following possible activities:



Ne^{23} and F^{20} decay by emitting a hard beta ray with a 1.63-Mev gamma ray following the beta ray from F^{20} . The Na^{22} activity would not be troublesome because the half-life is long and the activation cross-section is relatively small compared to that for the production of Na^{24} . In the case of Na^{24} there are two gamma rays with energies 2.76 and 1.38 Mev in cascade following the beta ray. It is, therefore, of particular interest for shield design to know the amount of Na^{24} produced in a coolant of sodium at various depths of B_4C .

Since the spectrum of neutrons at various thicknesses of B_4C is only very poorly known, and since the absorption cross-section of sodium is likewise in doubt in the intermediate energy region, it is essential that the activation be measured using sodium itself in the B_4C sample. However, since the cross-section for absorption in sodium is low, the direct measurement is possible

only for small attenuations with the available neutron source strength. This difficulty has been mitigated by making the direct measurements utilizing the most sensitive technique, and by taking measurements with a BF_3 counter, which is, of course, much more sensitive, so that the direct data can be extrapolated on the basis of the counter response. The direct measurements are discussed first.

The activation of a sample of NaNO_3 was determined by measuring the gamma radiation with a scintillation detector. This detector permits counting the activity from large thick sources. The total intrinsic efficiency of a good NaI phosphor 1 in. long and $1\frac{1}{2}$ in. in diameter for the gamma rays from Na^{24} is about 0.3 to 0.5. In practice one must discriminate against the small pulses, which lowers the efficiency for detecting gamma rays by an appreciable factor. In these experiments the overall efficiency was determined with a source of Na^{24} whose absolute disintegration rate was known. The standard sources of Na^{24} were supplied by W. S. Lyon of the Chemistry Division. The sources are standardized with a 4π ionization chamber calibrated as a function of gamma-ray energy. The absolute disintegration rate of the Na^{24} samples used in these experiments should not have an error more than 3%.

The sodium samples in the form of NaNO_3 crystals were exposed for from 8 to 50 hr to the neutron spectrum existing behind various depths of solid B_4C in the lid tank. The B_4C samples in the form of 1-in. slabs were placed in the two dry tanks which were followed by H_2O . For the preliminary experiments the NaNO_3 was placed in an aluminum tube of 1-in. diameter and $1/32$ -in. wall. This tube of NaNO_3 was then placed inside the B_4C counter jacket, and the jacket was placed in the water and against the dry tank.

After exposure the samples were dissolved in H_2O and counted with the scintillation detector. Each sample, containing 32.9 g of sodium in 200 ml of solution, was counted in a lucite tank surrounding the sides and top of the NaI phosphor. The standard sources of sodium used to calibrate the detector were counted under the same conditions.

In order to eliminate a difficulty in positioning the NaNO_3 during exposure the samples were packaged in an aluminum container 15 by 15 by $\frac{1}{4}$ in. with a $1/32$ -in. wall and placed between the 1-in. slabs at selected intervals. This arrangement proved successful. The results are given in Table 1. It appears, however, that the boundary of the inner and outer dry tanks introduces a discontinuity due to the approximately 1.3 cm of H_2O between the dry tanks.

As was expected, the presence of water greatly increased the sodium activation in its immediate vicinity. When several more centimeters of boron carbide was added, however, the effect was to reduce activation of the sodium, since the water is a more effective shield than the B_4C for the neutron spectrum penetrating the B_4C . There is an uncertainty of the order of 10 to 20% in the measurements, since the amount of H_2O present could not be accurately determined owing to its peculiar shape.

Sodium activation was measured directly in the B_4C at locations from 2 to 15 in. from the fission source. A few measurements of the activation of sodium were also obtained at various depths of $B_4C + Fe + B_4C$, since the effect of structural material should also be known.

The BF_3 counter was approximately 25 in. long and 2 in. in diameter. The counter was placed in a B_4C jacket which shielded the counter on five sides with 3 in. of B_4C (density 1.90 g/cc, water content 1.4% by weight) and on one side with 1 in. of B_4C . The B_4C was contained by an aluminum can $\frac{1}{4}$ in. thick over the exterior of the B_4C and $\frac{1}{8}$ in. thick over the interior. The counter could be used with either the 1-in. or the 3-in. side facing the source.

Measurements with the 25-in. BF_3 counter were taken throughout 40 in. of B_4C , but electronic difficulties were encountered which made the low counting-rate results uncertain. The measurements are being remade, and the data will be reported later.

The macroscopic cross-section of the BF_3 in the counter is 0.0329 cm^{-1} for thermal neutrons and the volume is 1.114 liters. On the basis of relative thermal-neutron capture cross-sections of BF_3 and sodium, the ratio of sodium activation per gram per second to counts per minute on the BF_3 counter would be 5.3×10^{-6} . However, the data indicate that this number is too low by a factor of about 5.0, probably because of resonance absorption in sodium.

There might be some question as to whether a boron counter in a boron shield would accentuate the valleys in the cross-section. For this reason another set of measurements was made using gold foils, for which the activation cross-section is quite well known in the intermediate energy region.⁽¹⁾

The gold foils were mounted and exposed on the aluminum facings of the B_4C slabs. They were then counted on a standard Geiger-Mueller counter. The results are reported in terms of thermal flux as determined in a graphite standard pile, but, since the spectrum in the B_4C differs considerably from that encountered in a graphite pile, the actual flux in the B_4C is very difficult to estimate.

(1) Henkel, R. L., and Barschall, H. H., "Capture Cross Sections for Fast Neutrons," *Phys. Rev.* 80, 145 (1950).

Biological Dose Behind B₄C-H₂O Shield. The distribution of thermal-neutron flux in H₂O behind various thicknesses of B₄C is reported in Table 3. Analysis of these data yields an effective fast-neutron removal cross-section for boron, from which the attenuation of any amount of B₄C in a hydrogenous shield can be computed.

The theory on which this computation is based predicts that the location of the B₄C within the shield does not affect the attenuation. To test this point a series of measurements were made in which 12 in. of B₄C was moved successively to several distances from the source. In the region from 80 to 160 cm from the source in the water the flux was observed to be invariant with respect to the B₄C position. This would, of course, not be the case if the B₄C were moved too near to the observation point, since spectrum transition effects would be predominant.

Traverse measurements were made behind both the dry tank (12 in. B₄C) and the 20-in. block to determine the extent of the streaming in from air voids which were inadvertently left beneath the samples. The results, given in Tables 6 and 7 and Figs. 7 and 8, indicate no serious perturbation as far as the thermal-neutron centerline distribution in H₂O was concerned. However, the voids did seriously affect the jacketed-counter measurements, and these are being rerun.

The gamma dose was measured behind various thicknesses of B₄C in water using an air-filled graphite-wall ionization chamber; the results are presented in Table 8. The apparent absorption coefficient of the B₄C for the gamma rays which are hard enough to penetrate 100 g/cm² of H₂O in addition to the B₄C is 0.0354 cm²/g. This is slightly less than the value obtained for water at this attenuation.

Measurements of preliminary mock-ups of the submarine shield containing Fe, B₄C, and H₂O in varying thicknesses are presented in Tables 9 and 10 and Figs. 10 and 11. As would be expected, replacing boron carbide with iron decreased the fast neutrons transmitted because of the high inelastic scattering cross-section of the latter. However, with respect to gamma attenuation, the iron is relatively inefficient at this position in the shield. This is expected because of the capture gamma rays from capture in iron of the intermediate-energy neutrons which build up in and penetrate both B₄C and Fe.

TABLE 1

Comparison of Na and Au Activation with BF_3 Counter Measurements in Solid B_4C Containers Fe, Al, H_2O ; NaNO_3 samples, 140 g; Au foils, ~ 0.005 in., 6.45 cm^2 ;25-in. BF_3 proportional counter, B_4C jacket

B_4C THICKNESS, $\rho = 2.3$ (cm)	Na ACTIVATION, R_0^*		B_4C THICKNESS, $\rho = 2.3$ (cm)	Au ACTIVATION (nv $\times 10^4$)**	B_4C THICKNESS,** $\rho = 2.3$ (cm)	25-in. BF_3 COUNTER (counts/min)
	Run 1	Run 2				
3.9	455		2.0	15.31	8.3	7.48×10^6
5.9	375	375	4.1	7.55	10.3	5.34×10^6
7.8	187		6.1	5.05	12.4	3.51×10^6
12.0	95.4		8.1	3.52	14.3	2.385×10^6
18.1	34.8		10.1	2.37	16.4	1.595×10^6
18.1	33.2	34.0	12.2	1.72	30.2	1.335×10^5
20.0			14.1	1.15	30.2	7.42×10^4
22.0	16.6		16.1	0.824	30.2	5.85×10^4
23.9	8.5		18.1	0.608		
23.9	11.2	10.6	20.2	0.414		
25.7	5.2		22.2	0.319		
27.8	3.4		24.2	4.30		
29.9		2.0	26.3	0.110		
			28.1	0.061		
			30.1	1.098		

* $R_0 = \text{Na}^{24}$ disintegrations per second per gram of sodium at saturation.

**The nv unit does not apply rigorously since the flux detected by the gold foils is not thermal.

***Including B_4C in jacket.

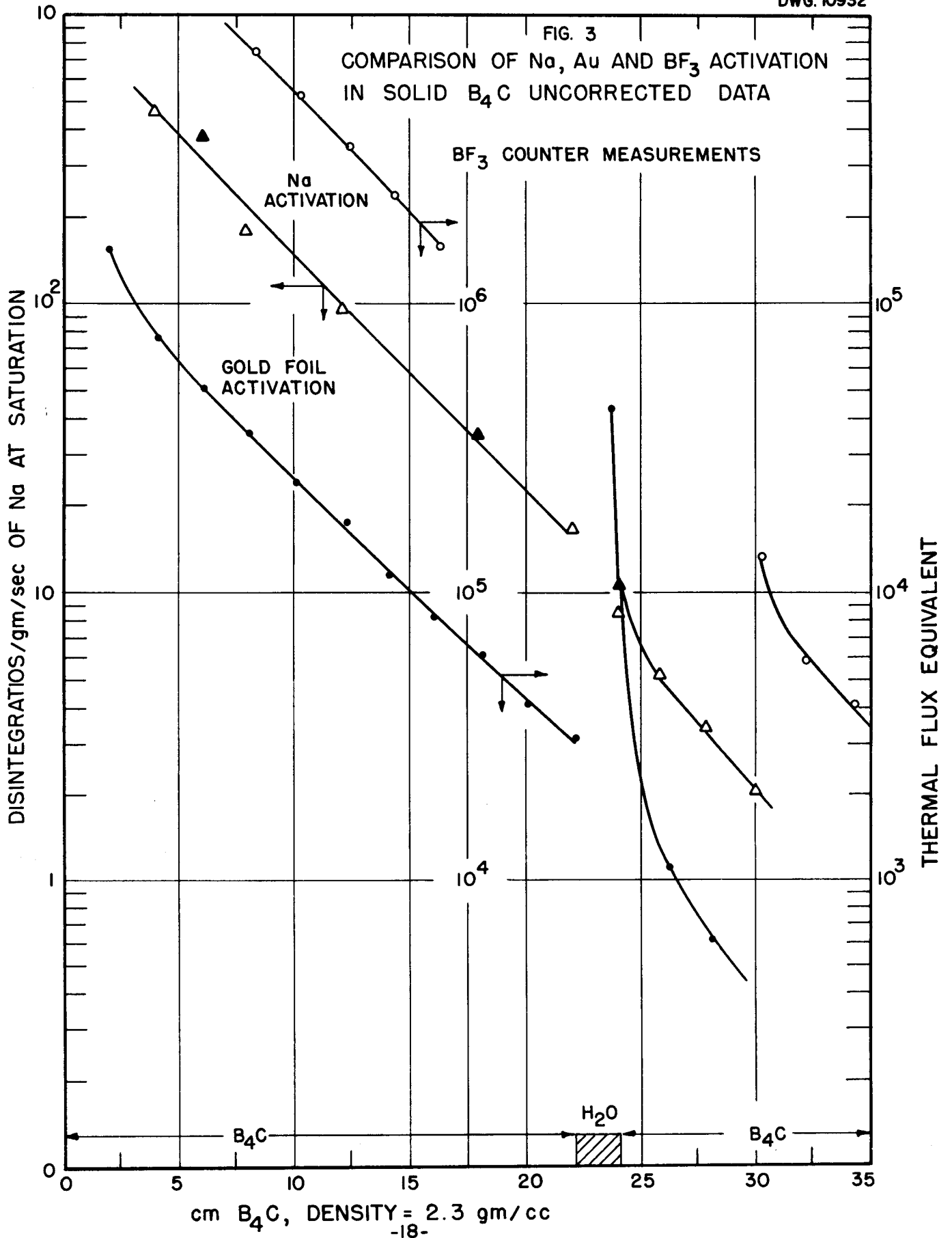
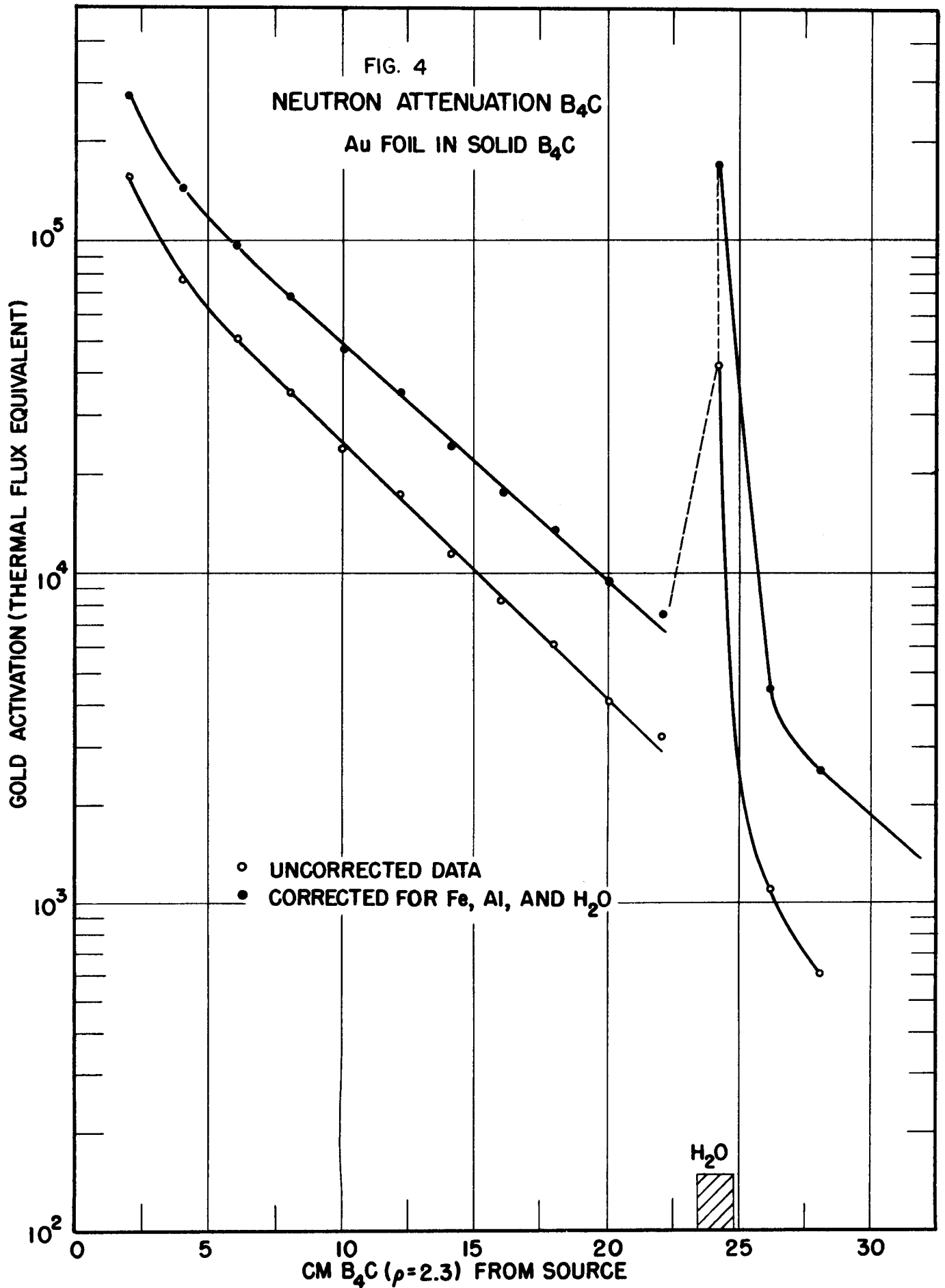


TABLE 2

Neutron Attenuation of B₄CCenterline measurements; Au foils placed in solid B₄C

THICKNESS OF B ₄ C ($\rho = 2.3$) BETWEEN FOIL AND SOURCE (cm)	Au FOIL ACTIVATION ($nv \times 10^4$)*	THICKNESS, t , OF Al BETWEEN FOIL AND SOURCE (cm)	Al CORRECTION FACTOR, $e^{0.085t}$	Au ACTIVATION CORRECTED FOR ATTENUATION OF Al, Fe, AND H ₂ O** ($nv \times 10^4$)*
2.0	15.31	0.315	1.026	27.47
4.1	7.55	0.630	1.054	14.00
6.1	5.05	0.945	1.082	9.55
8.1	3.515	1.260	1.111	6.82
10.1	2.37	1.575	1.140	4.74
12.3	1.72	1.890	1.171	3.53
14.1	1.15	2.205	1.202	2.42
16.1	0.824	2.520	1.234	1.78
18.1	0.608	2.835	1.266	1.35
20.2	0.414	3.150	1.300	0.942
22.2	0.319	3.465	1.335	0.745
24.2	4.30	3.780	1.368	17.08
26.3	0.110	4.095	1.407	0.449
28.1	0.061	4.410	1.445	0.255
30.1	1.098	4.725	1.484	4.79

*The nv units would apply only if flux were thermal.**Fe, H₂O correction factor for 0 through 20.19 cm of B₄C = 1.75; for 20.19 through 30.10 cm of B₄C = 2.90.



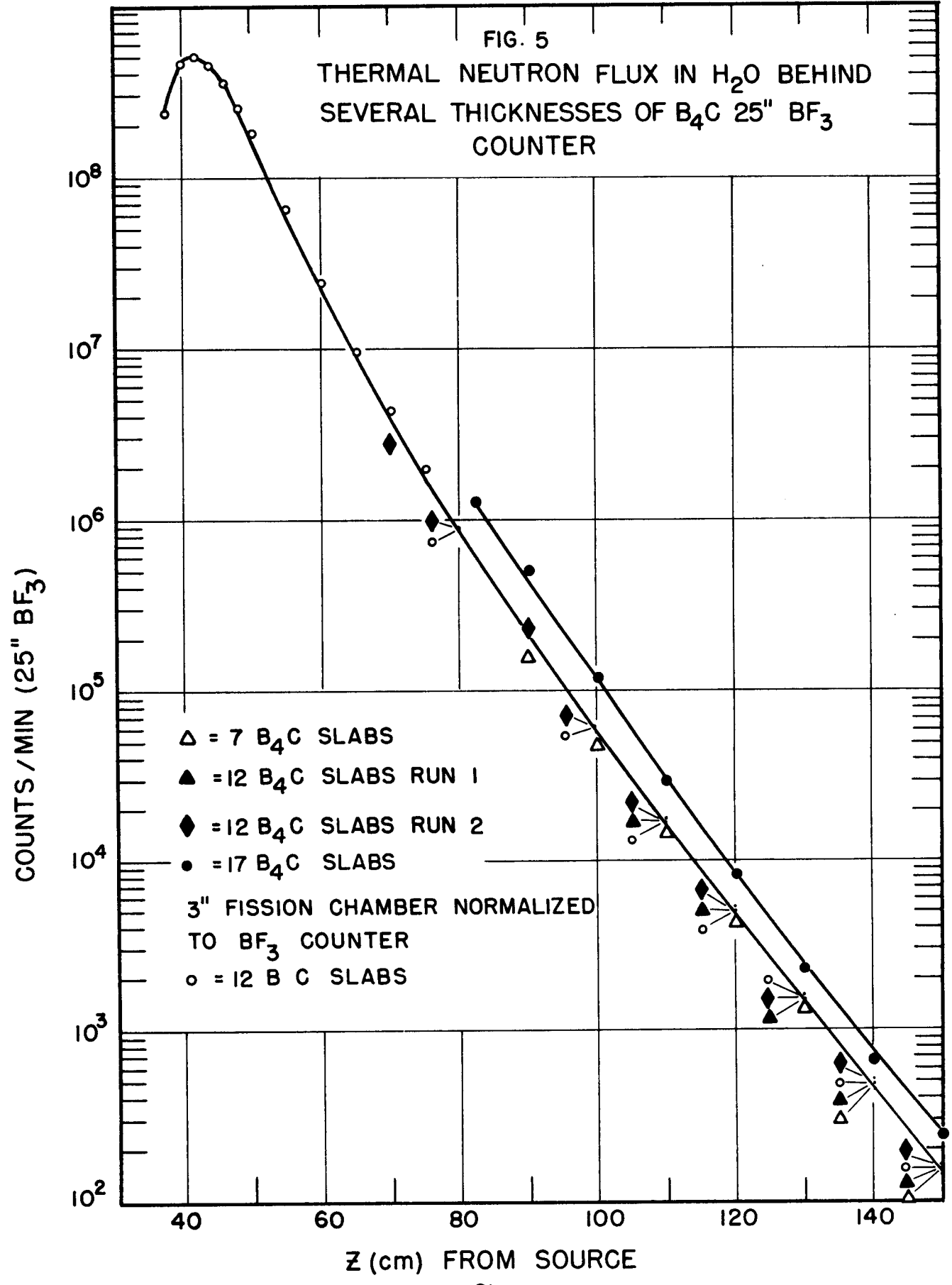


TABLE 3

Neutron Attenuation in H₂O Behind B₄CThermal-neutron centerline measurements; 25-in. BF₃ counter in H₂O behind solid B₄C

7 B ₄ C SLABS**		12 B ₄ C SLABS**			17 B ₄ C SLABS**	
z cm FROM SOURCE	(counts/min)	z cm FROM SOURCE	(counts/min)		z cm FROM SOURCE	(counts/min)
			RUN 1	RUN 2		
90	159.7 × 10 ³	70		2.72 × 10 ⁶	82.4	1.34 × 10 ⁶
100	48.30 × 10 ³	80		8.90 × 10 ⁵	90	5.06 × 10 ⁵
110	13.6 × 10 ³	90		2.34 × 10 ⁵	100	1.20 × 10 ⁵
120	4.21 × 10 ³	100		61.7 × 10 ³	110	28.9 × 10 ³
130	1.31 × 10 ³	110	17.17 × 10 ³	16.9 × 10 ³	120	7.97 × 10 ³
140	0.449 × 10 ³	120	5.06 × 10 ³	5.09 × 10 ³	130	2.16 × 10 ³
150	0.151 × 10 ³	130	1.52 × 10 ³	1.54 × 10 ³	140	0.665 × 10 ³
160	0.478 × 10 ²	140	0.490 × 10 ³	0.500 × 10 ³	150	0.231 × 10 ³
		150	0.160 × 10 ³	0.167 × 10 ³	160	0.84 × 10 ²
		160		0.578 × 10 ²		

*Voids under sample.

**B₄C slabs 2.54 cm thick; density ≈ 1.81 g/cc + 0.315 cm of aluminum per slab.

TABLE 4

Neutron Attenuation of $B_4C-H_2O^*$ 12 B_4C slabs; ** thermal-neutron centerline measurements

z cm FROM SOURCE	3-in. FISSION CHAMBER		25-in. BF_3 COUNTER, RUN 3 (counts/min)
	(counts/min)	(counts/min normalized to 25-in. BF_3 counter)	
37.8	83.5×10^3	2.28×10^8	
40	164.6×10^3	4.50×10^8	
42	185.0×10^3	5.06×10^8	
44	165.9×10^3	4.53×10^8	
46	129.4×10^3	3.535×10^8	
48	90.7×10^3	2.48×10^8	
50	64.3×10^3	1.76×10^8	
55	23.3×10^3	6.37×10^7	
60	8.78×10^3	2.40×10^7	
65	3.50×10^3	9.56×10^6	
70	1.57×10^3	4.28×10^6	
75	0.717×10^3	1.96×10^6	
80	0.320×10^3	0.874×10^6	
100			58.6×10^3
110			16.4×10^3
120			4.87×10^3
130			1.50×10^3
140			0.479×10^3
150			0.158×10^3

*No voids.

** B_4C slabs 2.54 cm thick; density ≈ 1.81 g/cc + 0.315 cm of aluminum per slab.

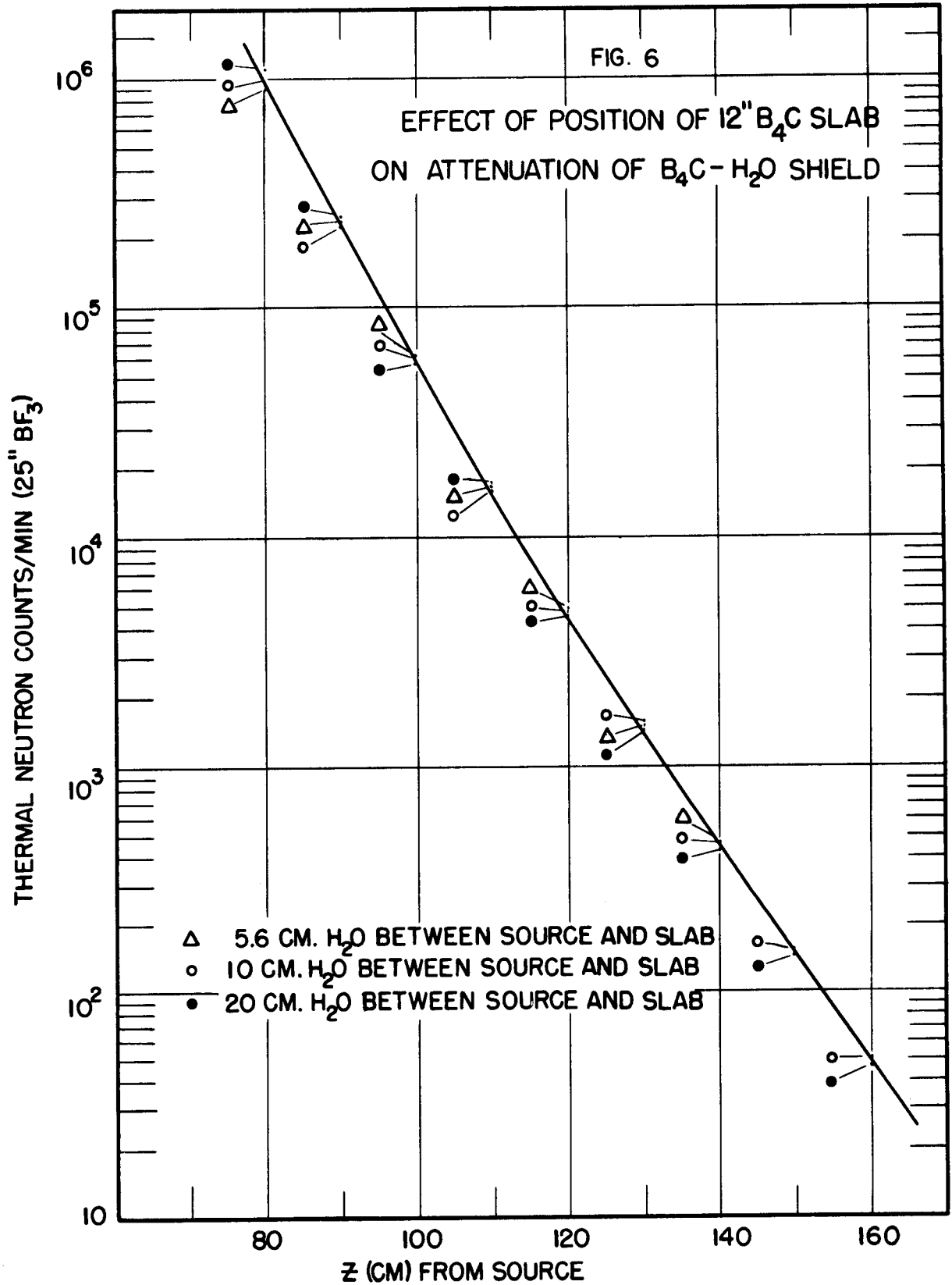


TABLE 5

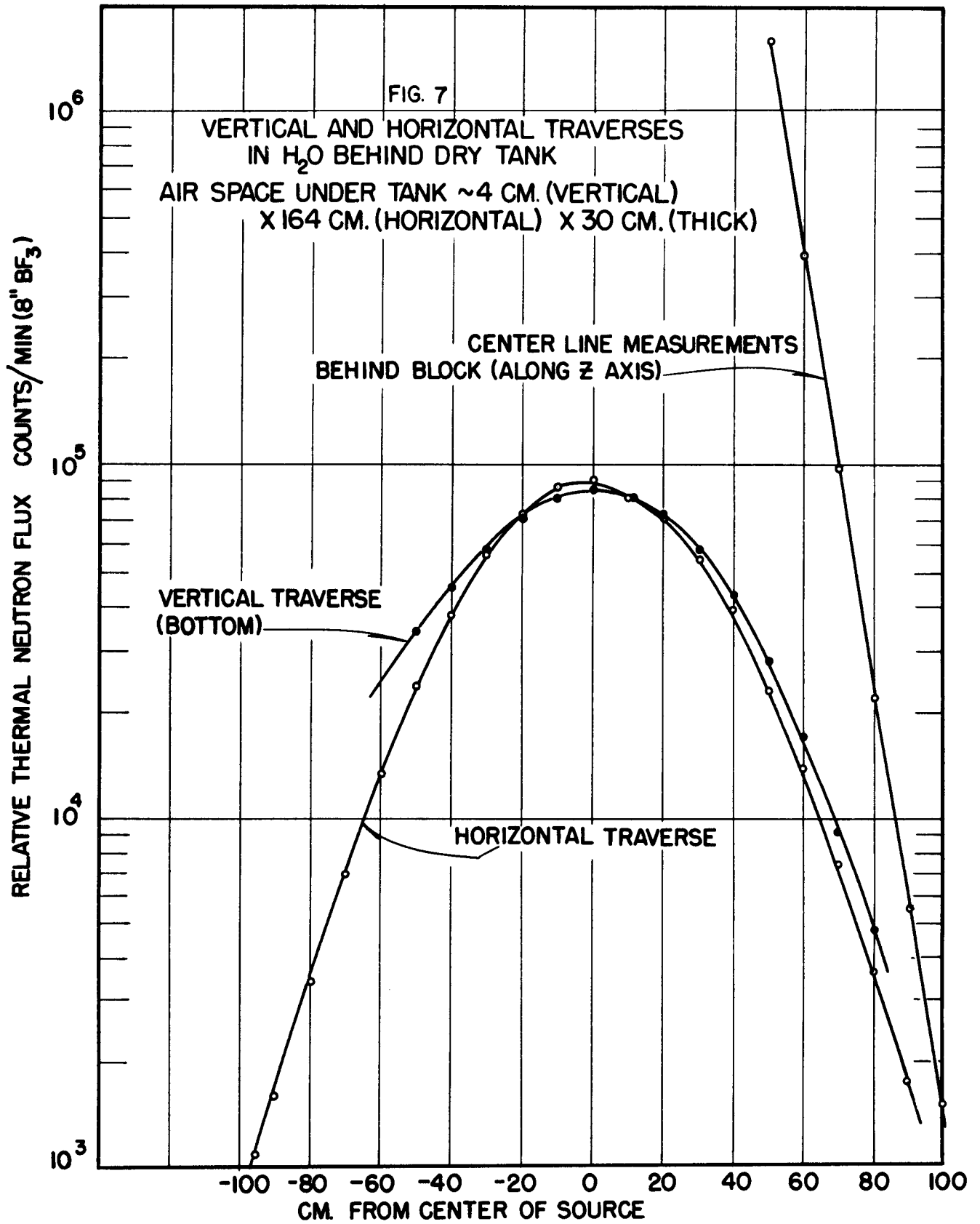
Effect of Position of 12-in. B_4C Slab on Attenuation of B_4C-H_2O Shield

Thermal-neutron centerline measurements; 25-in. BF_3 counter in H_2O behind solid B_4C

12 B_4C SLABS,* 5.6 cm OF H_2O BETWEEN SOURCE AND TANK** HOLDING SLABS		12 B_4C SLABS,* 10.0 cm OF H_2O BETWEEN SOURCE AND TANK** HOLDING SLABS		12 B_4C SLABS,* 20.0 cm OF H_2O BETWEEN SOURCE AND TANK** HOLDING SLABS	
z cm FROM SOURCE	(counts/min)	z cm FROM SOURCE	(counts/min)	z cm FROM SOURCE	(counts/min)
80	9.05×10^5	80	9.17×10^5	80	10.58×10^5
90	2.36×10^5	90	2.335×10^5	90	2.42×10^5
100	61.25×10^3	100	59.8×10^3	100	59.4×10^3
110	17.2×10^3	110	16.6×10^3	110	16.6×10^3
120	4.95×10^3	120	4.80×10^3	120	4.70×10^3
130	1.465×10^3	130	1.47×10^3	130	1.44×10^3
140	0.486×10^3	140	0.458×10^3	140	0.448×10^3
		150	0.153×10^3	150	0.150×10^3
		160	0.514×10^2	160	0.468×10^2

* B_4C slabs 2.54 cm thick; density ≈ 1.81 g/cc + 0.315 cm of aluminum per slab.

**Total outside thickness of tank = 35.6 cm; both tank walls = 0.63 cm of Fe.



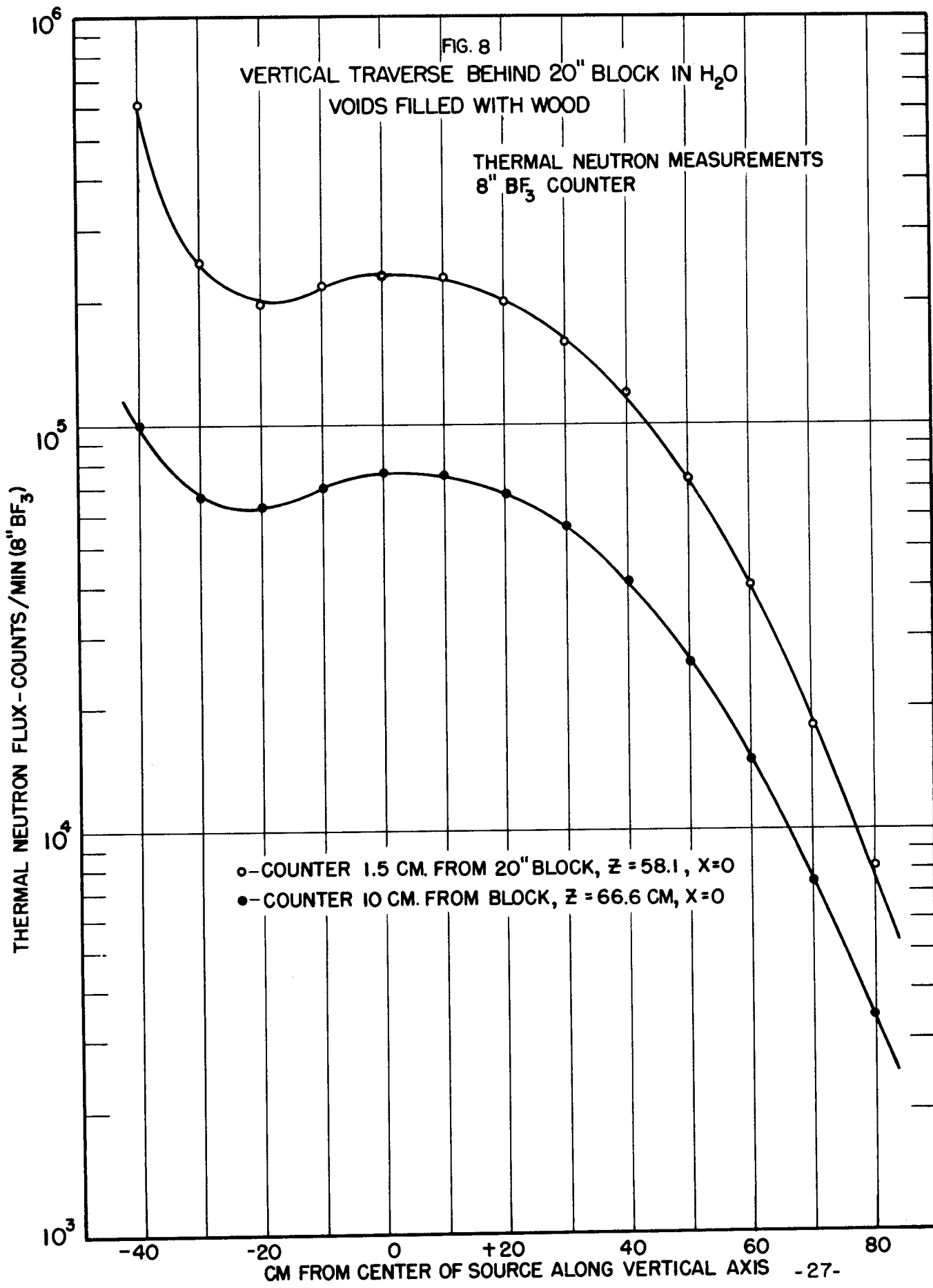


TABLE 6

Vertical and Horizontal Traverses in H₂O Behind B₄C in Dry Tank*

Thermal-neutron measurements; 8-in. BF₃ counter in H₂O behind solid B₄C;
7 B₄C Slabs** from z = 2 cm to z = 22 cm

CENTERLINE MEASUREMENTS z = 0, y = 0		HORIZONTAL TRAVERSE z = 70 cm, y = 0		VERTICAL TRAVERSE z = 70 cm, x = 0	
z cm FROM SOURCE***	(counts/min)	x cm FROM z AXIS	(counts/min)	y cm FROM z AXIS	(counts/min)
50	15.98 × 10 ⁵	+90	1.75 × 10 ³	+80	4.77 × 10 ³
60	3.95 × 10 ⁵	+80	3.68 × 10 ³	+70	9.07 × 10 ³
70	89.7 × 10 ³	+70	7.41 × 10 ³	+60	16.6 × 10 ³
80	21.6 × 10 ³	+60	14.0 × 10 ³	+50	27.9 × 10 ³
90	5.51 × 10 ³	+50	23.5 × 10 ³	+40	42.8 × 10 ³
100	1.53 × 10 ³	+40	39.4 × 10 ³	+30	58.4 × 10 ³
		+30	54.4 × 10 ³	+20	71.98 × 10 ³
		+20	70.2 × 10 ³	+10	81.3 × 10 ³
		+10	81.5 × 10 ³	0	84.7 × 10 ³
		0	91.4 × 10 ³	-10	80.7 × 10 ³
		-10	87.4 × 10 ³	-20	71.1 × 10 ³
		-20	73.2 × 10 ³	-30	58.2 × 10 ³
		-30	56.4 × 10 ³	-40	45.2 × 10 ³
		-40	38.4 × 10 ³	-50	34.3 × 10 ³
		-50	24.3 × 10 ³		
		-60	13.6 × 10 ³		
		-70	6.96 × 10 ³		
		-80	3.43 × 10 ³		
		-90	1.61 × 10 ³		
		-95	1.06 × 10 ³		

*Air space under dry tank, y = -50 to -54; z = 4 to z = 34; x = -82 to 82 cm.

**B₄C slabs 2.54 cm thick; density ≈ 1.81 + 0.315 cm of aluminum per slab.

***z axis is perpendicular to the plane of the source; y = 0 and x = 0 at its center.

TABLE 7

Vertical Traverse Behind 20-in. B₄C Block in H₂OVoids filled with wood; thermal-neutron measurements; 8-in. BF₃ counter

20 in. B ₄ C, COUNTER 10 cm FROM 20-in. B ₄ C BLOCK $x^* = 0, z = 66.6$ cm		20 in. B ₄ C, COUNTER 1.5 cm FROM 20-in. B ₄ C BLOCK $x^* = 0, z = 54.6$ cm	
y TRAVERSE (cm)	(counts/min)	y TRAVERSE (cm)	(counts/min)
+80	3.36×10^3	+80	8.12×10^3
+70	7.41×10^3	+70	18.3×10^3
+60	15.4×10^3	+60	40.3×10^3
+50	26.8×10^3	+50	73.8×10^3
+40	41.0×10^3	+40	1.17×10^5
+30	56.0×10^3	+30	1.64×10^5
+20	68.1×10^3	+20	2.01×10^5
+10	75.6×10^3	+10	2.27×10^5
0	76.0×10^3	0	2.33×10^5
-10	70.2×10^3	-10	2.20×10^5
-20	63.0×10^3	-20	1.99×10^5
-30	67.5×10^3	-30	2.53×10^5
-40	100.5×10^3	-40	6.09×10^5

* x axis is horizontal, z axis is perpendicular to source at $x = 0, y = 0$.

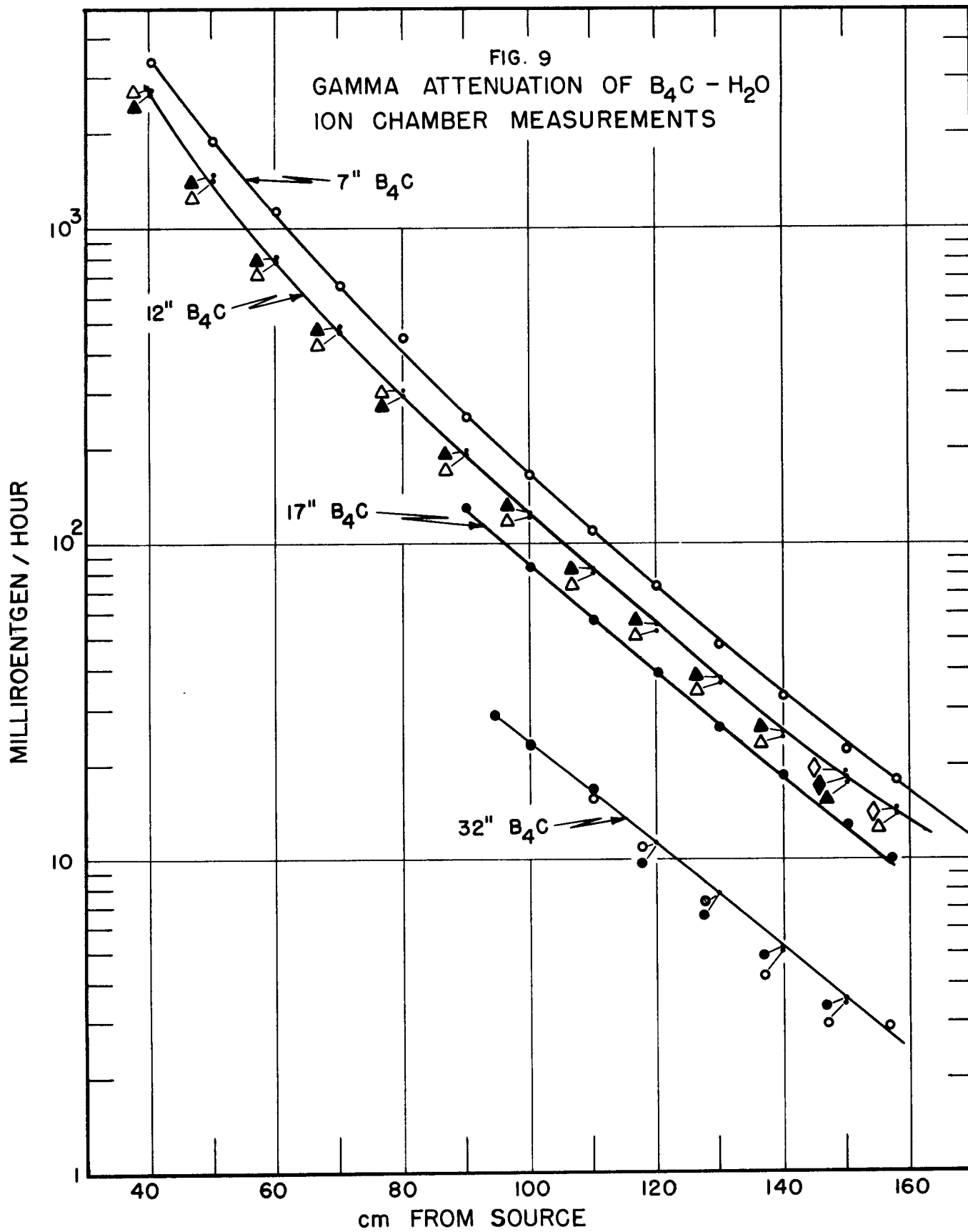


TABLE 8
Attenuation of B_4C-H_2O

Gamma centerline measurements; 10^{10} and 10^{12} ionization chambers

z cm FROM SOURCE	(milliroentgen/hour)							
	7 B_4C SLABS* + $\frac{1}{4}$ in. Fe,	12 B_4C SLABS* + $\frac{1}{4}$ in. Fe				17 B_4C SLABS* + $\frac{1}{4}$ in. Fe,	12 B_4C SLABS + 20 in. B_4C ** + $\frac{1}{4}$ in. Fe	
	RUN 1	RUN 1	RUN 2	RUN 3	RUN 4	RUN 1	RUN 1***	RUN 2***
39.6			2713					
40.0			2716					
40.5	3335	2581						
41.2								
50	1890	1475	1418					
60	1120	805	771					
70	656	484	468					
78.6						219		
80	450	290	299			201		
90	253	194	189			131		
94.3							28.8	
100	163	126	121			84.4	23.4	
110	86.8	82.3	80.0			57.0	16.6	15.6
115								
120	72.1	55.5	52.4			38.8	11.0	11.1
130	47.7	37.1	35.9			26.3	7.81	7.77
140	32.7	25.0	24.5			18.5	5.41	5.03
150	22.3	17.2	17.1	18.0	18.5	12.8	3.52	3.47
157				4.0		10.0		2.92
157.7	17.7	13.8			14.4	0		

* B_4C + Al = 5.45 g/cm²/slab, Al = 0.85 g/cm²/slab.

**20-in. block = 97.03 g/cm² B_4C , 9.91 g/cm² Fe, 6.9 g/cm² H₂O.

***Runs 1 and 2 were made in water containing 0.5% boron.

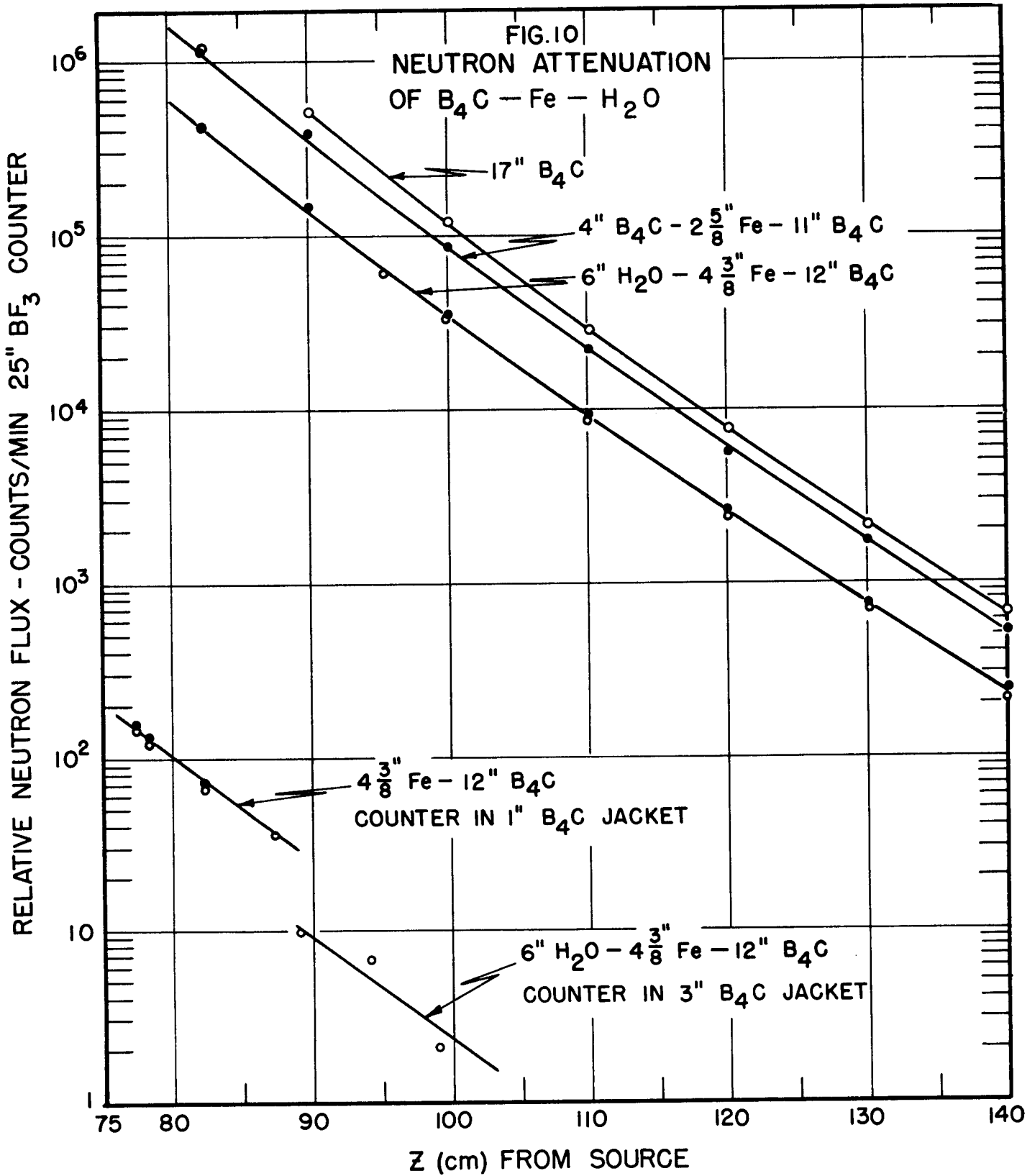


TABLE 9

Neutron Attenuation of B_4C -Fe- H_2O 25-in. BF_3 counter in H_2O behind solid B_4C slabs + Fe*

4 B_4C , 3 Fe,* 11 B_4C SLABS		5 Fe, 12 B_4C SLABS		15 cm H_2O ; 5 Fe, 12 B_4C SLABS		5 Fe, 12 B_4C SLABS; 25-in. BF_3 COUNTER IN B_4C JACKET; 1-in. B_4C SIDE FACING SOURCE			15 cm H_2O ; 5 Fe, 12 B_4C SLABS 25-in. BF_3 COUNTER IN B_4C JACKET; 3-in. B_4C SIDE FACING SOURCE	
z cm FROM SOURCE	(counts/min)	z cm FROM SOURCE	(counts/min)	z cm FROM SOURCE	(counts/min)	z cm FROM SOURCE	(counts/min)		z cm FROM SOURCE	(counts/min)
							RUN 1	RUN 2		
82.3	11.38×10^5	82.3	4.23×10^5	95.4	60.8×10^3	77.3	143.0	150.8	89	10.0
90	3.95×10^5	90	1.49×10^5	100	34.7×10^3	78.3	127.7	137.0	94	6.91
100	88.4×10^3	100	33.7×10^3	110	8.86×10^3	82.3	69.8	76.8	99	2.10
110	22.2×10^3	110	9.36×10^3	120	2.43×10^3	87.3	37.0			
120	5.76×10^3	120	2.58×10^3	130	0.720×10^3					
130	1.72×10^3	130	7.49×10^2	140	0.212×10^3					
140	0.510×10^3	140	2.38×10^2							
150	0.167×10^3	150	0.81×10^2							

* B_4C slabs are 2.54 cm thick, with density $\approx 1.81 + 0.315$ cm of aluminum; Fe slabs are 2.22 cm thick, mild steel.

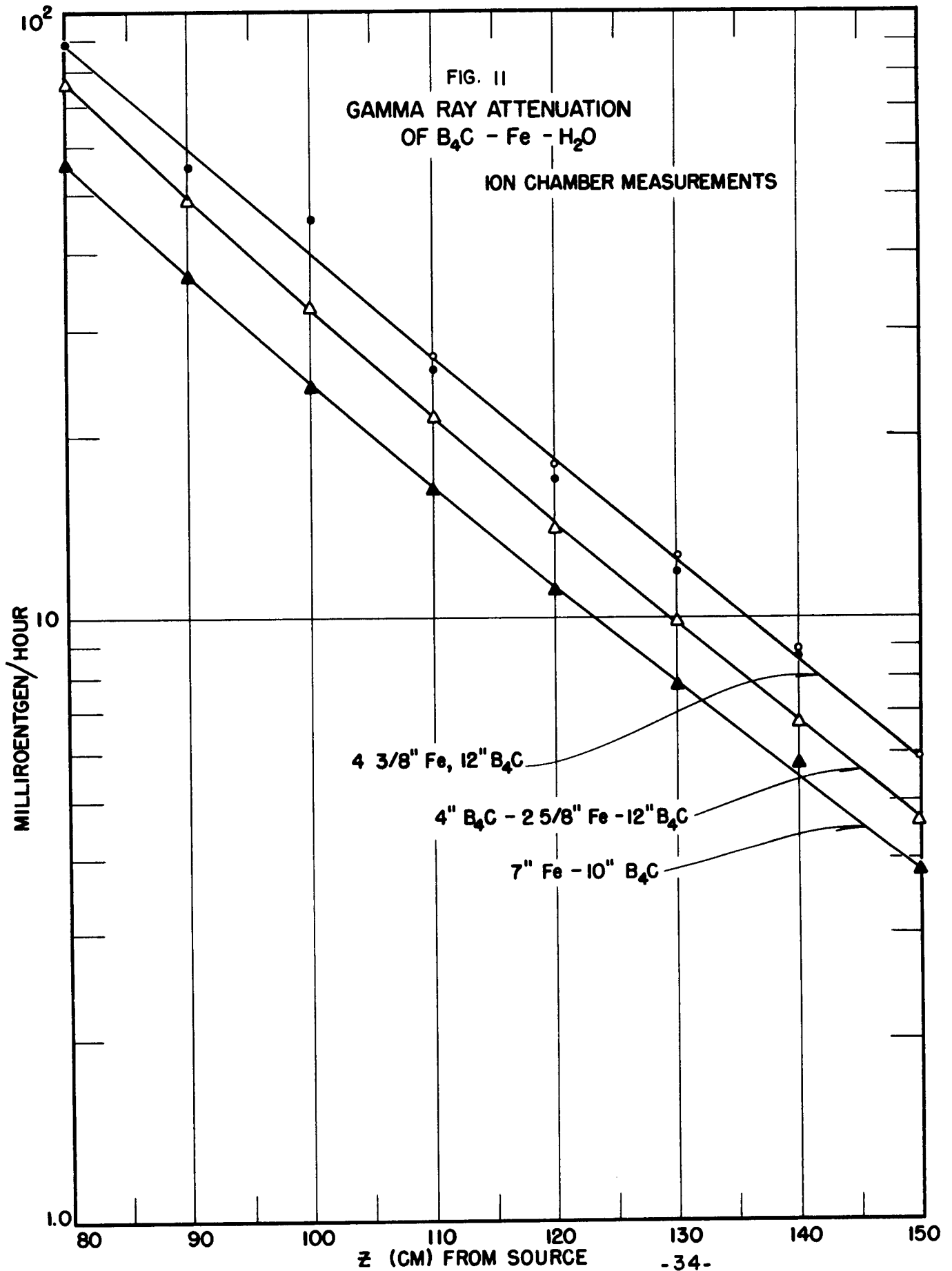


TABLE 10
Gamma Ray Attenuation of B₄C, Fe, and H₂O
 10¹⁰ and 10¹² ionization chambers

z cm FROM SOURCE	(milliroentgens/hour)			
	4 B ₄ C, 3 Fe, 11 B ₄ C, RUN 1	5 Fe, 12 B ₄ C		8 Fe, 10 B ₄ C, RUN 1
		RUN 1	RUN 2	
80	76.2	88.6		55.9
90	48.7	55.3		36.3
100	32.4	45.6		24.0
110	21.4	25.9	27.1	16.3
120	14.0	17.0	17.9	11.1
130	9.79	12.0	12.7	7.71
140	6.67	8.63	8.85	5.72
150	4.59		5.91	3.81
157			4.65	

3. LIQUID-METAL DUCT TEST

R. Lewis M. K. Hullings
C. Clifford M. C. Marney
 L. Frankwitz*

The liquid-metal duct test being conducted in the water tank on the thermal column is designed primarily to determine transmission of neutrons down a coolant duct. Measurements of the neutron intensities in the water beyond the end of several lengths of duct are being taken with gold and indium foils and with a BF_3 counter. The ducts consists of two concentric steel pipes of 6 and 8 in. I. D. Straight sections and sections with one and two 90° bends are being used in the measurements. The following duct configurations have been measured:

1. A straight section 24 in. long inclined at 36° from the source plane and air filled.
2. Same as above with a 4-in. B_4C jacket on the outside pipe.
3. Same as item 1 with inner pipe filled with aluminum powder to a density of 0.97 g/cc; this density was decided upon by the KAPL Physics Division on the basis of neutron cross-sections for sodium and aluminum.
4. A straight section 24 in. long followed by a 90° bend on a 6-in. radius (axis length = 9.4 in.) followed by a straight section 18 in. long, all air filled.
5. Same as item 4 with the inner pipe filled with aluminum.

These measurements will be continued and further measurements on a duct with two 90° bends with the various configurations will also be measured. Details of the experiment and most recent results are reported in ANP quarterly reports (e.g., ORNL- 919, ANP-60).

4. BULK SHIELDING TEST FACILITY

J. L. Meem

The progress made in the new facility is reported in detail in the current ANP quarterly report (ANP-60). Calibration of the measuring instruments has been completed although the absolute value of the thermal-neutron calibrations is subject to change. The final value depends on the new figure which will result from the calibration of the graphite sigma pile by E. D. Klema. The power calibration of the shielding reactor is about 75% complete.

Centerline measurements in pure water are 90% completed. Immediately, upon completion of these measurements, fast-neutron dosage measurements on an iron-water shield of interest to the submarine project is proposed. These measurements should delay the tests on the unit shield by a maximum of two weeks. The unit shield tests are now scheduled to start in early April.

A list of the spectroscopic instruments under development for the divided-shield measurements is given in the ANP quarterly report (ANP-60).

5. ANP PHYSICS GROUP

Only a summary is given here of the work done by this group during the past quarter; a detailed report may be found in the ANP quarterly report (ANP-60).

The IBM Fermi-diffusion multigroup calculational procedures have come into fruition through the cooperative effort of the ANP Physics Group and the Uranium Control and Computing Section of Y-12. The productive capacity of this operation, now some 13 reactors a week, has materially advanced the capabilities of the group in the survey of reactor characteristics and, in keeping up with the engineering variations and the shifts of interest.

The development of the IBM calculations has not followed a smooth course, however, since some three weeks of calculational time was lost in locating and rectifying a mathematical source of divergence in the flux solutions.

Since the original interest of the ANP Project was in liquid-metal-cooled solid-fuel reactor designs, the first calculations produced concerned this class of reactors. The "statics," i.e., the critical mass, flux distribution, etc., of these models apply almost equally well to liquid-fuel designs provided they have the same median energy of fission. The solid-fuel studies are reported in some detail, followed by a description of the ANP liquid-fuel 200-megawatt design of Jan. 9, 1951. It so happens that the median energy of fission of the latter (18 ev) is somewhat less than that of the solid-fuel designs (70 ev) because of difference in moderator percentages.

The solid-fuel reflected reactor calculations are of interest in that they show the effect on criticality, critical mass, etc. brought about by the change of several important parameters, as follows:

1. The change of moderator from beryllium oxide to beryllium which is shown to give a substantial increase in reactivity.
2. The effect on criticality and critical mass of changes of density, coolant, and moderator.
3. The effect of changing the reflector thickness.
4. The effect of replacement of beryllium oxide reflector with a nonmoderated stainless steel reflector, which is shown to decrease criticality.

5. The effect of xenon poisoning.
6. The effect of heterogeneity of uranium lumping.
7. The effect of iteration of the source term.

Following a routine investigation of the ANP liquid-fuel design of January 9 by means of study of the equivalent bare reactor, IBM calculations of reflected reactors were undertaken. A series of calculations was made which enable the estimation of the kinetic temperature coefficient of reactivity.

The kinetics of the liquid-fuel reactor has been the subject of a large amount of investigation, which has revealed the desirability of a short thermal relaxation time of the fuel tubes and of a long neutron lifetime. The worst types of accidents to which the nuclear-powered aircraft may be subjected are thought to be (1) the failure of two turbojet motors, or (2) the failure of one-third of the primary coolant lumping power. Neither one of these failures is sufficient to make the reactor go into prompt-critical condition. In consideration of the time required for failure and the presence of delayed neutrons it results that the self-regulation of the reactor to the emergency changes is well-damped and safe. Calculations of the behavior of the reactor in the absence of damping effect of the delayed neutrons indicate that the reactor would safely regulate changes which might even throw it slightly prompt critical.

With the change of emphasis of the engineering studies to the Aircraft Reactor Experiment, bare-reactor studies of the proposed ARE designs were begun. It was desired that the ARE would possess as many as possible of the kinetic characteristics of the high-powered 200-megawatt ANP reactor. This resulted in a dilemma from which one could emerge only through arbitrary decision. A design of the ARE possessing exactly the same characteristics of the ANP would have insufficient fuel volume for criticality. This results even though the critical mass of the ARE is much reduced because of its increased moderator volume percentage. It has been necessary to increase the size of the fuel tubes, thereby increasing the thermal relaxation time, and to increase the number of fuel tubes to the desired quantity; however, since the ARE is more nearly thermal, the increase of neutron lifetime tends to offset the departure from ideal equivalents.

Reflected ARE calculations have begun, but reportable results are not available.

[REDACTED]

The kinetic response of the proposed ARE designs have been studied and compared with that response of the ANP design. It has been found that a broad region of acceptable designs exists.

Calculation of the critical mass expected from the current beryllium-uranium-aluminum assemblies of Callihan's group has been undertaken. It is found that the calculations have overestimated the critical mass by some 50% of the true value. In view of the experience of other groups in the first estimation of critical masses from fundamental data this result is not too surprising. Investigation of the sources of error are proceeding, and a number of small discrepancies between the experimental set-up and the calculations have been discovered but none sufficient to account for the large divergence. Obviously some time and further experimentation will be necessary before theoretical and experimental values will come into agreement. It should be our goal to calculate critical masses by the modified Fermi-diffusion method to about 25%. It may not be practical at this time to attempt to improve calculations beyond this point.